

Identification of Bodner-Partom model parameters for technical fabrics

P. Kłosowski^a, K. Żerdzicki^a, K. Woźnica^b

^a Gdansk University of Technology, Faculty of Civil and Environmental Engineering, ul. G. Narutowicza 11/12, 80-233 Gdansk, Poland

^b Institut National des Sciences Appliquées Centre Val de Loire, Laboratoire PRISME, 88 Boulevard Lahitolle, 18000 Bourges, France

abstract

The thorough analysis of modeling technical fabrics behavior with the viscoplastic Bodner-Partom constitutive law is presented. The study has been focused on differences between the warp and weft direction of the material. To obtain the model's parameters only the uniaxial tensile laboratory tests with three different, but constant strain rates are required. The parameters have been found for polyester fibers PVC coated fabrics: VALMEX and AF9032, respectively. An extensive attention has been paid to the behavior of the textile in the weft direction, therefore for this direction the supplementary cyclic tests have been performed and analyzed. Consequently, the same identification procedure for the warp and weft direction of the fabric, taking into account the appropriate longitudinal stiffness, has been successfully implemented. Two new approaches for the weft threads direction description have been proposed. All identification results have been examined through computer simulations producing sound convergence with the laboratory results for both analyzed materials.

Keywords: Fabrics, Mechanical properties, Analytical modeling, Viscoplastic behavior, Bodner-Partom model

1. Introduction

Architectural fabrics generally consist of the following components: base fabric (polyester or glass fiber yarns), adhesive coat, exterior coating (PVC, PTFE) and top coating [27]. The yarns are responsible for the tensile strength of the material, while exterior coating protects yarns from damage, stabilizes weave structure, as well as provides waterproofing and shear stiffness. Due to these facts the base fabric threads and exterior coating are taken into the mechanical analysis of technical fabrics. The investigation can be carried out at three levels of accuracy [18]: at macro-, meso- and micro-level. Many researchers have developed the analytical models of the meso-structure, describing yarns response under uniaxial and biaxial loading [23,15,9,22,2].

The discrete models and over-detailed continuum approaches require large computational capabilities and are time-consuming. They are not suitable for calculations of large civil constructions, like roof structures or building facades made of textiles [15,29]. Therefore, the continuum models with the basic comprehension of the meso-structure processes are sufficient for civil applications [10,29]. These models take into account the mechanical properties of perpendicular yarns families and capture change of the angle between threads at each step of deformation. Hence, they generally need only stress-strain relations in the warp and weft direction

separately, which can be easily established by uniaxial and biaxial tests. The constitutive models initially destined for metals have also been used in this studies. The creep potential model with three orthotropic parameters has been investigated upon the polyethylene terephthalate fabric coated with the PVC [14]. For modeling the time-dependent and rheological properties of fabrics the viscoplastic models of Bodner-Partom and Chaboche have been also successfully applied in [16], where the authors have analyzed the technical fabric PANAMA, which is composed of plain weaved (P 2/2; according to DIN 61 101) polyester threads both sides PVC coated. Their work has been limited to identification of the Bodner-Partom model parameters for the warp direction. On the assumption that the fabric threads in both orthogonal directions are made from the same material and have the same density and micro-structure the authors have also adopted the parameters determined for the warp yarns into the analysis of the weft yarns behavior.

According to current research, the procedure [16] mentioned above is not always sufficient for a comprehensive description of the fabrics functioning. That is usually complicated, as architectural fabrics belong to the very particular group of composite materials. When the physical properties of yarns in both directions are not the same, or when the threads weaving method is sophisticated, then the mechanical properties of the material should be determined for each fabric direction individually. In the present paper two types of polyester fibers PVC coated fabrics have been analyzed. The study concerns the uniaxial properties of these materials, as

they can be easily extrapolated for the biaxial case. First time, it has been proven by Reinhardt [24] that uniaxial strength is equal to the biaxial one for polyester fibers PVC coated fabrics. Then, this observation has been confirmed for polyarylate fiber polyurethane coated membrane for the case of samples (uniaxial and biaxial) with open-hole [19]. Additionally, this investigation has revealed that open-hole strength of the analyzed fabric is approximately independent of the warp/weft load ratio in the biaxial tests. The most recent experimental studies on AF9032 polyester fibers PVC coated fabric have shown, that the uniaxial results can be directly used for description of the biaxial behavior of the material, especially at the preliminary design stage of membrane structures [3]. It has been also confirmed, that strain-stress curves of biaxial tests seems to be independent of the warp/weft load ratio (apart from ratios higher than 1:8 and 8:1) and are still very close to the ones obtained for the uniaxial cases. The present research includes the analysis of polyester fibers PVC coated fabrics (VALMEX and above mentioned AF9032), thus it has been decided to focus only on the response of the architectural fabrics under uniaxial loading. Special attention has been paid to a profound insight into the weft direction elasto-viscoplastic characteristics of the textile, as experimentally obtained strain-stress curves tend to be complex.

2. Bodner-Partom constitutive model

The Bodner-Partom constitutive equations have been originally proposed by Bodner and Partom in 1975 for the nonlinear elastic viscoplastic strain-hardening response prediction for a titanium alloy [6]. In the following several years the Bodner-Partom model has been refined to take into account the kinematic and thermal recovery [21], as well as damage effects [7]. During the last 40 years the basic formulations have been extended through advanced computing implementations [26,4], various modifications [30,11] and wider applications especially for non-metallic materials such as polymers [30], living tissues [25,20] and architectural fabrics [16,30]. The Bodner-Partom model is willingly employed for material description, because it requires only a few parameters, which can be obtained from uniaxial tensile tests through quite simple identification procedure.

In the Bodner-Partom formulation it is assumed that the inelastic effects starts from the beginning of the deformation, thus the total strain rate $\dot{\epsilon}$ is additively decomposed on elastic $\dot{\epsilon}_e$ and inelastic $\dot{\epsilon}_p$ strain rate components:

$$\dot{\epsilon} = \dot{\epsilon}_e + \dot{\epsilon}_p \quad (2.1)$$

The Bodner-Partom model in the case of uniaxial monotonic tension without recovery effects can be described by the following expression:

$$\dot{\epsilon}_p = \frac{2}{\sqrt{3}} D_0 \exp \left[-\frac{1}{2} \left(\frac{R+D}{\sigma} \right)^{2n} \frac{n+1}{n} \right] \text{sgn}(\sigma); \quad (2.2)$$

where $\dot{\epsilon}_p$ is the inelastic strain rate, σ stands for stress, D_0, n are the model parameters, the isotropic (R) and kinematic (D) hardening functions are described by the set of evolution equations and are generally presented in a saturation-type format with prescribed initial conditions:

$$\begin{aligned} \Delta\sigma &= E(\Delta\epsilon - \Delta t \dot{\epsilon}_p); \quad \sigma = \sigma + \Delta\sigma \\ \dot{W}^I &= \sigma \dot{\epsilon}_p; \\ \dot{R} &= m_1(R_1 - R)\dot{W}^I; \quad R(0) = R_0; \\ \dot{X} &= m_2 \left(\sqrt{3/2} D_1 \text{sgn}(\sigma) - X \right) \dot{W}^I; \quad X(0) = 0; \\ D &= \sqrt{2/3} X \text{sgn}(\sigma); \end{aligned} \quad (2.3)$$

The kinematic hardening rate function \dot{X} refers to the stress level and depends also on the kinematic hardening X and the plastic work W^I . The parameters m_1 and m_2 are saturation rate coefficients of the isotropic and kinematic hardening respectively, and $\Delta\epsilon$ is the increment of the total strain between two following load increments. The integration of formula (2.3) gives the hardening functions in the following forms:

$$\begin{aligned} R &= R_1 [1 - \exp(-m_1 W^I)] + R_0 \exp(-m_1 W^I); \\ X &= \sqrt{3/2} D_1 \text{sgn}(\sigma) [1 - \exp(-m_2 W^I)]; \\ D &= D_1 [1 - \exp(-m_2 W^I)]; \end{aligned} \quad (2.4)$$

The relation between stress σ , inelastic strain rate $\dot{\epsilon}_p$, temperature T and hardening variables R, D can be demonstrated as the functional f_1 , which is the combination of the Prandtl-Reuss law and some parts of the kinetic equations and is given in the general formula as:

$$\frac{\sigma}{R+D} = f_1(\dot{\epsilon}_p, T) \quad (2.5)$$

For the Bodner-Partom formulation (Eq. (2.2)) the functional f_1 can be expressed as follows:

$$f_1 = \left[\frac{2n}{n+1} \ln \left(\frac{2D_0}{\sqrt{3}\dot{\epsilon}_p} \right) \right]^{-\frac{1}{2n}} \quad (2.6)$$

All the parameters of the Bodner-Partom model and their units adapted for technical fabrics are compiled in Table 1. More detailed explanation of the Bodner-Partom constitutive model, its wider mathematical description and different loading examples can be found in [7,4,11,25,17].

3. Experiments

3.1. Samples

Two types of technical fabrics have been used in this study: VALMEX and AF9032. The viscoplastic parameters identified for these textiles have been compared to the technical fabric PANAMA [16] (the same type of fabric). The producer's specifications of the coated fabrics under investigation are listed in Table 2.

All examined fabrics are built of polyester fibers and are both sides coated with PVC. They have also similar thickness of about 1 mm. The core difference between two analyzed textiles can be

Table 1
Bodner-Partom model's parameters with units for technical fabrics.^a

Parameter	Units	Description
E	kN/m	Young's modulus
ν	-	Poisson's modulus
m_1	[kN/m] ⁻¹	Coefficient for isotropic hardening
m_2	[kN/m] ⁻¹	Coefficient for kinematic hardening
A_1	s ⁻¹	Recovery rate coefficient for isotropic hardening
A_2	s ⁻¹	Recovery rate coefficient for kinematic hardening
D_0	s ⁻¹	Limiting (maximum) strain rate
R_0	kN/m	Initial value for isotropic hardening
R_1	kN/m	Limiting (maximum) value for isotropic hardening
R_2	kN/m	Fully recovered (minimum) value for isotropic hardening
D_1	kN/m	Limiting (maximum) value for kinematic hardening
n	-	Strain rate sensitivity parameter
r_1	-	Recovery exponent for isotropic hardening
r_2	-	Recovery exponent for kinematic hardening

^a As usually for technical fabrics, due to difficulties with thickness measurements, all mechanical properties in this paper are defined for the unitary thickness e.g. kN/m² · m = kN/m.

Table 2
Production properties of analyzed technical fabrics.

Trade Name of fabric	PANAMA	Valmex FR 1000 Hallentype III Universal	Shelter-Rite AF9032
Trademark Holder/Supplier	Sattler Company	Mehler Company	Seaman Corporation
Base fabric weight	275 g/m ²	(no data)	339 g/m ²
Finish fabric weight	870 g/m ²	1200 g/m ²	1085 g/m ²
Weave style	Basket weave (Panama; 2/2)	Plain weave	Weft-inserted warp-knit
Fibers	Polyester	Polyester	Polyester
Coating	PVC	PVC	PVC
Strip tensile warp/weft	420/400 daN/5 cm	550/550 daN/5 cm	578/578 daN/5 cm

found in their weaving structure (VALMEX – plain weave, AF9032 – weft-inserted warp-knit) resulting in probably different stress distribution in the material under subjected force, especially in the weft direction. The fabric's producers have not specified whether the fabric has been pre-stressed in the weft direction during coating process, what is important in the investigation of fabric behavior.

The dimensions of the specimens have been chosen according to ISO 1421 (2001) national standard [13]. The width of a specimen was 50 ± 0.5 mm, while the grip separation (specimen active length) was 200 ± 0.5 mm.

3.2. Uniaxial tensile tests

The identification of the Bodner-Partom model's parameters requires only uniaxial tests with different but constant strain rates. The tensile testing has been conducted with selected strain rates of 0.005, 0.001 and 0.0001 1/s, up to rupture. The experiments have been carried out at room temperature on the Zwick Roell Z020 strength machine. The actual distance between gauge points has been constantly recorded by the video-extensometer with the precision of 0.001 mm. The gauge length (different for each test) of the device has been used as a base of strain calculations. For each strain rate in the warp and weft direction at least 3 tests have been carried out. The representative stress-strain curves obtained for different strain rates for the coated fabric VALMEX and AF9032 are depicted in Fig. 1.

It can be observed that the plots for both fabrics are similar in shape, despite the fact, that analyzed textiles have the different types of weaving structure. It may be concluded, that both fabrics have been treated (pre-stressed) in the same way during coating process. The following significant finding proves that both coated fabrics exhibit rate-dependent behavior, what may be a prerequisite to use one of the viscous constitutive models for the performance description of these particular textiles. In this work, the analysis has been carried out on the assumption of the permanent inelastic elongations of fabrics under high (close to admissible) loads. It also takes into account a viscoplastic effects, therefore the Bodner-Partom model has been implemented. This model also permits the analysis of dynamic loads cases and allows studying behavior of the material above yield limit, that is useful in the modeling of damage processes.

4. Parameters identification

4.1. Longitudinal stiffness

In the beginning, the inclinations of linear parts of the experimental stress-strain curves have been identified by the multi-

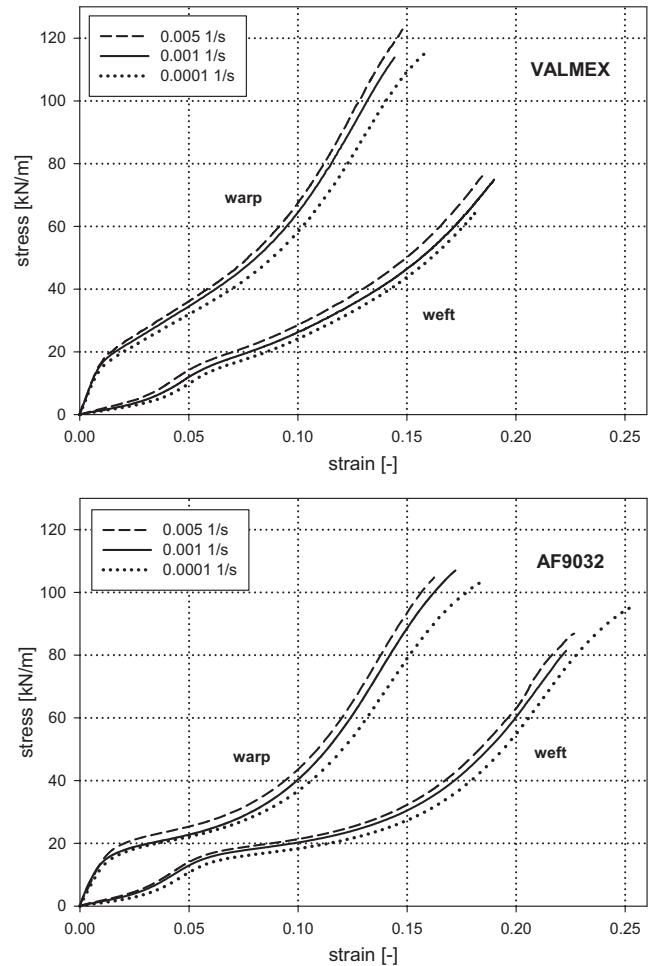


Fig. 1. Typical stress-strain curves for the technical fabrics VALMEX and AF9032 for different strain rates in uniaxial tensile tests.

step linear approximation. For the warp direction two (E_{w1}^{VAL} , E_{w1}^{AF} , where VAL = VALMEX, AF = AF9032 and $i = 1, 2$) and for the weft direction three (E_{fj}^{VAL} , E_{fj}^{AF} , where $j = 1, 2, 3$) inclination coefficients of characteristic linear sections have been determined (Fig. 2).

They represent the longitudinal stiffness values in the specific sections of the stress-strain curves. The intersections points (ε_0 ; $\varepsilon_{1/2}$; $\varepsilon_{2/3}$; ε_F) have been calculated resulting in the applicability ranges of the particular longitudinal stiffness values. This method has been applied to the experimental data of both yarns' directions for each strain rate. The final values of longitudinal stiffness and intersection points have been calculated as the mean value of three strain rates. The results of this investigation are compiled in Table 3 in the form of the arithmetic mean value \bar{x} and \pm its standard deviation \bar{s}_x .

The study of the fabrics behavior has been limited to the strain level of 0.05 in the warp, and to the strain level of 0.1 in the weft direction (due to the Bodner-Partom model assumptions). This restriction is applied due to the practical and designing reasons. These elongations correspond to the acceptable level of stresses and geometrical requirements usually practiced in civil engineering structures.

When comparing both materials it is clearly seen that for the warp direction both stiffness coefficients of coated fabric AF9032 (E_{w1}^{AF} , E_{w2}^{AF}) are much lower than for the coated fabric VALMEX (E_{w1}^{VAL} , E_{w2}^{VAL}). The evaluation of the weft direction results reveals that

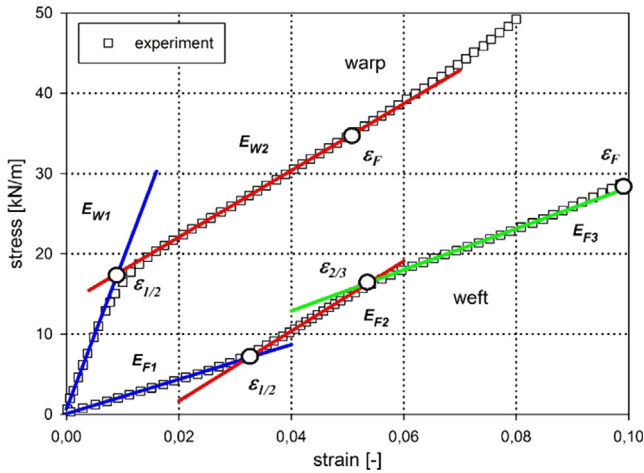


Fig. 2. Stress-strain curve of technical fabric VALMEX with characteristic linear sections for strain rate of 0.005 1/s.

the first stiffness moduli are almost the same (E_{F1}^{VAL} , E_{F1}^{AF}), the second are quite close to each other (E_{F2}^{VAL} , E_{F2}^{AF}), while the greatest discrepancy is found between the third moduli of interest (E_{F3}^{VAL} , E_{F3}^{AF}).

4.2. Approximation of experimental data

During the initial part of the tensile test, the weft threads undergo straightening, as they are primarily crimped due to weaving in the fabric manufacturing process. As a consequence, for the weft direction the first stiffness modulus (E_{F1}), limited to about 2.5% of the strain range, is mainly related to the mechanical properties of coating (PVC) and the slippage of the not tensioned weft threads, and for that reason, cannot represent the stiffness modulus for the whole fabric in the weft direction. The domain E_{F2} stands for the state, where threads are fully straightened and carry subjected force.

To study this problem the cyclic tests in elastic domain have been conducted. The initial range of strains is presented in Fig. 3, where the loading of VALMEX fabric to the particular level of stress (corresponding to the stiffness modulus E_{F1} and E_{F2} domain, respectively) and then unloading with the recovery time of about 120 s is plotted. In both cases the strain level has decreased to about 1%.

The elongations of the samples have been checked also after 3 days, giving the permanent strain level of about 0.2%. These results have confirmed that VALMEX coated fabric behavior for small strains can be described as viscoelastic. The dependence of the stiffness modulus on the stress and strain level is also clearly

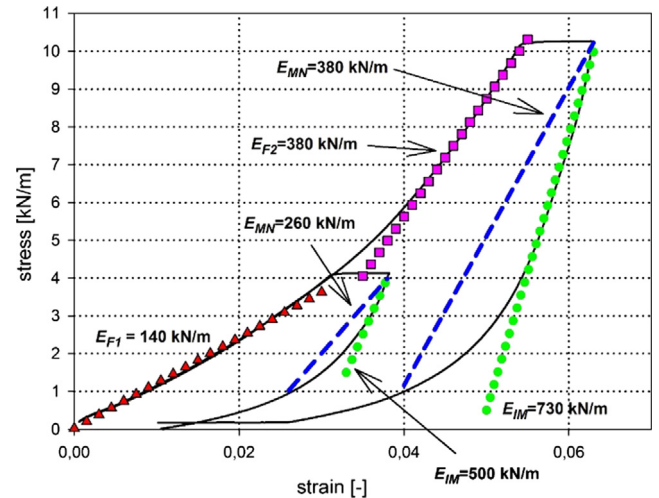


Fig. 3. Unloading tests for the weft direction of technical fabric VALMEX.

visible and proves that behavior in the lower stress levels is complex due to the combination of simultaneously acting: PVC covering and polyester base of composite fabric. Therefore, the terms of immediate E_{MN} and mean E_{MN} values of the stiffness modulus could be introduced. A similar phenomenon has been comprehensively studied in [5] for polyamide based woven strap samples used in cargo parachutes. In the present case, dotted lines in Fig. 3 represent immediate unloading moduli E_{MN} (identified as the tangential to the strain-stress curve at the beginning of unloading), while the short-dashed ones represent the mean unloading moduli E_{MN} , defined here as the secant line of the strain-stress curve between the start point of unloading and the stress level of 1 kN/m. The additional loading and unloading tests of the coated fabric VALMEX have been conducted with the constant strain rate of 0.001 1/s, with relaxation periods of 10 s only and with constant increase of peak strain level (of about 1.5%) in subsequent cycle (Fig. 4).

It has been observed that for lower stress level (<4 kN/m) the E_{MN} value is between values of E_{F1} and E_{F2} moduli and depends on the point when stresses increase again. For higher stress level (10 kN/m) the E_{MN} modulus corresponds to the E_{F2} modulus (Fig. 4). It has also been confirmed by the analysis of the inclination coefficients in the stress-strain plot for the loading and unloading stages (Fig. 4), where unloading modulus is always closer to the E_{F2} modulus.

Concluding, in the weft direction of VALMEX material the second stiffness modulus E_{F2}^{VAL} represents the true stiffness modulus. The same conclusion has been drawn for the coated fabric AF9032 under cyclic loading, including the uniaxial and biaxial cyclic tests, and is given in [1].

Table 3
Immediate non-linear longitudinal stiffness of technical fabrics.

Name	Longitudinal stiffness [kN/m]		Ranges of applicability			
			ε_0 [10^{-4}]	$\varepsilon_{1/2}$ [10^{-4}]	$\varepsilon_{2/3}$ [10^{-4}]	ε_F [10^{-4}]
VALMEX	E_{W1}	1830 ± 30	0	91 ± 3	-	-
	E_{W2}	420 ± 10	-	91 ± 3	-	500
	E_{F1}	140 ± 20	0	356 ± 21	-	-
	E_{F2}	380 ± 30	-	356 ± 21	576 ± 31	-
	E_{F3}	240 ± 10	-	-	576 ± 31	1000
AF9032	E_{W1}	1420 ± 80	0	118 ± 5	-	-
	E_{W2}	160 ± 10	-	118 ± 5	-	500
	E_{F1}	140 ± 20	0	281 ± 7	-	-
	E_{F2}	420 ± 10	-	281 ± 7	552 ± 13	-
	E_{F3}	100 ± 10	-	-	552 ± 13	1000

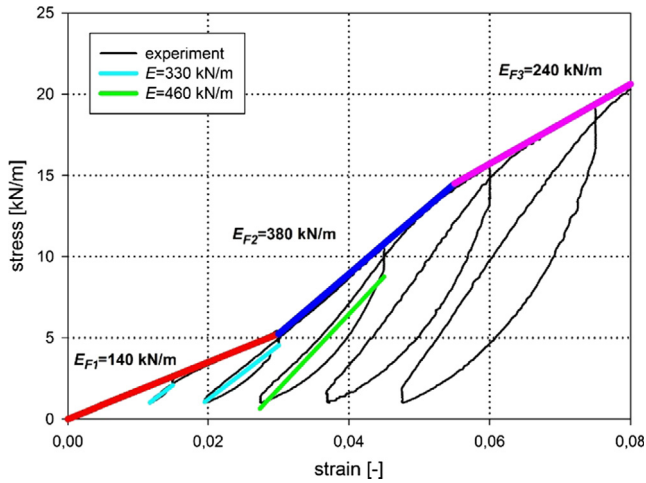


Fig. 4. Cyclic loading and unloading test for the weft direction of technical fabric VALMEX.

To sum up, the strain range corresponding to E_{F1} modulus is correlated to the initial stretching of the threads. It does not influence (or has very small influence on) the stress state and can be neglected, particularly when the architectural fabrics are pre-stressed during construction assembly. Therefore, in approximation of strain-stress curves, the first part of the data plot has been omitted (E_{F1}) and the value of E_{F2} has been assumed as the proper value of the stiffness modulus in the weft direction and has been used to shift the stress-strain curve (Fig. 5). The threads in the warp direction are generally pre-stressed in manufacturing process, so the value of E_{W1} has been used for the translation and further calculations (Fig. 5).

4.3. Identification procedure of Bodner-Partom model parameters

The Bodner-Partom model's parameters identification has been carried out according to the procedure earlier proposed in [11] for metals. For technical fabrics the identification procedure of that model has been presented in [16]. In that paper authors managed to give parameters for the warp direction and assumed that they are the same in the weft direction as both threads families are produced from the same material. In the present work the constitutive law parameters for architectural fabrics VALMEX and AF9032 have

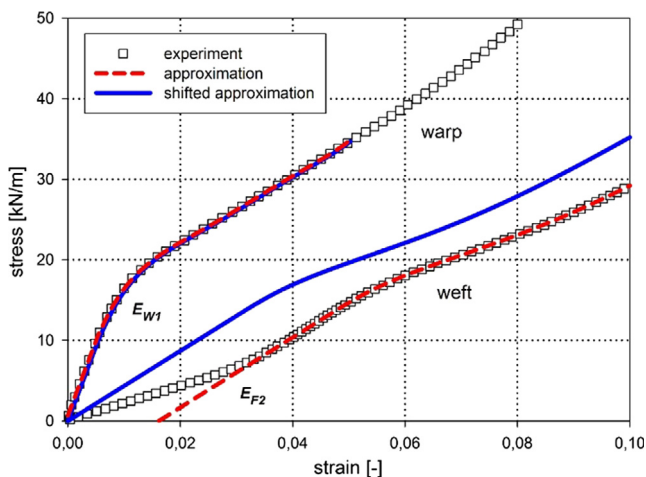


Fig. 5. Approximation of experimental data for the warp and weft direction of technical fabric VALMEX for strain rate of 0.005 1/s.

been determined for the warp and weft direction independently. It is possible due to the precise analysis of the material response under cyclic loading-unloading tests (for details see Section 4.2). As a result the appropriate longitudinal values of stiffness have been used for calculating the preliminary shifting of the experimental strain-stress curves, which in turn guaranteed correct model identification for the warp and weft direction individually.

In essence, the identification procedure of the Bodner-Partom model parameters has consisted of the following steps:

- Uniaxial tensile tests with at least three different but constant strain rates form the basis of the identification giving the stress-strain function $\sigma(\varepsilon)$ obtained for each strain rate separately.
- The stress-inelastic strain relation $\sigma(\varepsilon_p)$ is plotted and subsequently approximated by a chosen analytical function. For technical fabrics the following function can be used:

$$\sigma(\varepsilon_p) = a(1 - \exp(-b\varepsilon_p)) + c(1 - \exp(-d\varepsilon_p)) + f, \quad (4.1)$$

where the parameters a, b, c, d, f have been determined using the least square method in the Marquardt-Levenberg algorithm (Fig. 6).

- The work hardening rate $\dot{\gamma}$ can be calculated from the formula:

$$\dot{\gamma} = \frac{d\sigma}{dW_p} = \frac{d\sigma}{d\varepsilon_p} \cdot \frac{1}{\sigma}, \quad (4.2)$$

where the term $d\sigma/d\varepsilon_p$ is a derivative of the function given in Eq. (4.1). According to Eq. (2.3), it can be rewritten as:

$$\dot{\gamma} = f_1[m_1(R_1 - R) + m_2(D_1 - D)]. \quad (4.3)$$

- The work hardening rate $\dot{\gamma}$ is now drawn as the function of stress $\dot{\gamma}(\sigma)$. It allows to find the parameters m_2 and m_1 as the slopes of tangents to the curve for the beginning part of the plot corresponding to the small plastic strains ($\varepsilon_p = 0.2\%$), and in the range of the upper plastic strains ($\varepsilon_p = 2\%$), respectively (Fig. 7).
- The constant D_0 corresponds to the highest possible strain rate that can arise in the material. It is usually selected on the base of the literature study. For example, in [8,12] the parameter D_0 is set at $D_0 = 10^4 \text{ s}^{-1}$ for the average strain rate of 10 s^{-1} , while for the higher strain rates ($10^1 - 10^3 \text{ s}^{-1}$) $D_0 = 10^6 \text{ s}^{-1}$ is proposed. For the analysis of explosions it reaches even $D_0 = 10^8 \text{ s}^{-1}$.
- Combining Eq. (2.5) with Eq. (2.6) upon the assumption that at the beginning, at very low inelastic strains ($\varepsilon_p = 0.2\%$), the isotropic hardening is almost identical to its starting value $R \approx R_0$

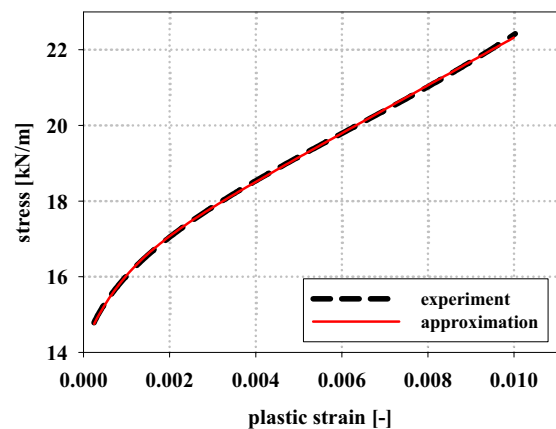


Fig. 6. Typical stress-plastic strain plot with approximation.

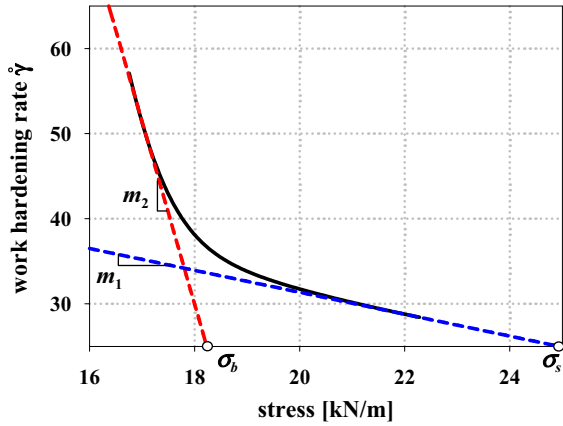


Fig. 7. Identification of parameters m_1, m_2 , and variables σ_b, σ_s .

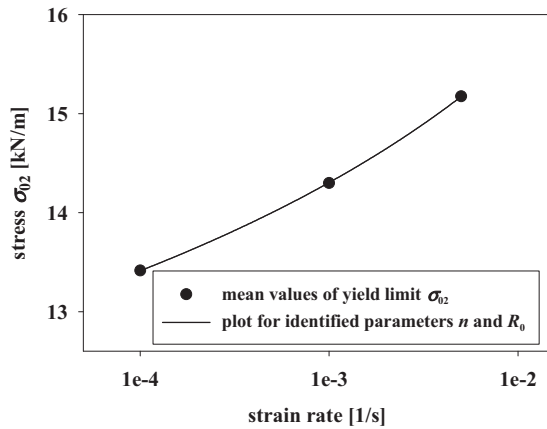


Fig. 8. Identification of the parameters n, R_0 .

and the kinematic hardening has not appeared yet (therefore $D \approx 0$), the technical yield limit σ_{02} for the Bodner-Partom model can be obtained in the form:

$$\sigma_{02} = \left[\frac{2n}{n+1} \ln \frac{2D_0}{\sqrt{3}\dot{\epsilon}_p} \right]^{-\frac{1}{2n}} R_0 \quad (4.4)$$

The values of σ_{02} are then determined for three different, but constant strain rates separately. After that, the relation (4.4) allows estimation of the parameters n and R_0 (Fig. 8).

- Supposing Eq. (4.3) for $\dot{\gamma} = 0$, the parameters D_1 and R_1 can be calculated from the equations:

$$\begin{aligned} D_1 &= \frac{m_2\sigma_b - m_1\sigma_s}{f_1(\dot{\epsilon}_{p02})(m_2 - m_1)} - R_0 \\ R_1 &= \frac{m_2\sigma_s - m_1\sigma_b}{f_1(\dot{\epsilon}_{p02})(m_2 - m_1)} + R_0 \end{aligned} \quad (4.5)$$

where σ_b and σ_s are the points at which tangents with m_2 and m_1 slopes, respectively, intercept the stress axis at the $\dot{\gamma}(\sigma)$ plot (Fig. 7).

The results of the identification for the warp and weft direction are presented in Table 4. For the coated fabric VALMEX the most important differences between the warp and weft direction are observed for parameters m_1 ($\sim 50\%$), n ($\sim 35\%$) and R_1 ($\sim 25\%$). For technical fabric AF9032 the parameter m_1 for both directions are almost the same, but other constants exhibit more discrepancies. Comparing analyzed textiles, it may be concluded that there is a general tendency among all identified constants. Parameters for the warp direction are permanently higher than the same ones for the weft direction, except for n parameter, which is lower for fabric AF9032.

5. Numerical simulations

The identification results have been verified by the numerical simulations of the laboratory tests using the determined material parameters and the software described in [28]. For the modeling of the weft direction response, obtained results have been applied in two ways. In the first one, only the longitudinal stiffness modulus E_{F2} has been taken into account, while in the second one the values of two moduli E_{F1} and E_{F2} have been implemented in the computer simulations, like in [16] for the study of technical fabric PANAMA. Fig. 9 presents the experimental results compared to the one- and two-modulus simulations for the strain rate of 0.0001 1/s. The results obtained for another strain rates are similar. The stress-strain functions for the warp direction are presented in Fig. 10, also giving great convergences with corresponding experimental curves.

For a comparison, the approach used in [16] for technical fabric PANAMA has also been adopted for the analysis of the coated fabrics VALMEX and AF9032. The parameters of the Bodner-Partom law obtained for the warp direction have also been used in the numerical simulations of the textiles behavior in the weft direction, however, with inclusion of E_{F1} and E_{F2} values determined for the weft direction (Fig. 11).

The correlation coefficients between the experimental results and the simulated curves have been also calculated. The best convergence is observed for the one modulus approach in the weft direction ($\bar{R}^2 = 0.99$), nevertheless, the other types of the analysis of the correlation coefficients are still satisfactory ($\bar{R}^2 = 0.95 \pm 0.98$). However, in the range of inelastic response (study Fig. 11), which starts beyond the applicability of E_{F2} , the warp direction parameters result in the higher trajectory of the simulating curve than for the weft direction parameters. As expected, coefficients originally recognized for the weft direction cause the appropriate inclination of the plot, which is closer to the test data. It is clearly seen here that the usage of parameters specified originally for the warp direction to calculate the behavior in the weft direction causes considerable discrepancies for both technical fabrics.

On the basis of the presented research it is suggested that the first section of the strain-stress curve for the weft direction can be neglected in the viscoplastic analysis of that type of material. Consequently, two applications of the identification results are proposed: the one-modulus and two moduli concept. In the first

Table 4
Bodner-Partom model's parameters identified for analyzed technical fabrics.

Name	Direction	m_1 [kN/m] ⁻¹	m_2 [kN/m] ⁻¹	D_0 [s ⁻¹]	D_1 [kN/m]	R_0 [kN/m]	R_1 [kN/m]	n [-]
VALMEX	Warp	0.83 ± 0.06	34 ± 1	1	3.0 ± 0.2	30	90 ± 7	1.9
	Weft	1.7 ± 0.2	27 ± 7	1	2.8 ± 0.8	31	72 ± 8	1.4
AF9032	Warp	0.58 ± 0.17	31 ± 3	1	4.8 ± 1.5	33	79 ± 7	1.4
	Weft	0.57 ± 0.10	23 ± 2	1	2.7 ± 0.2	24	48 ± 4	2.2

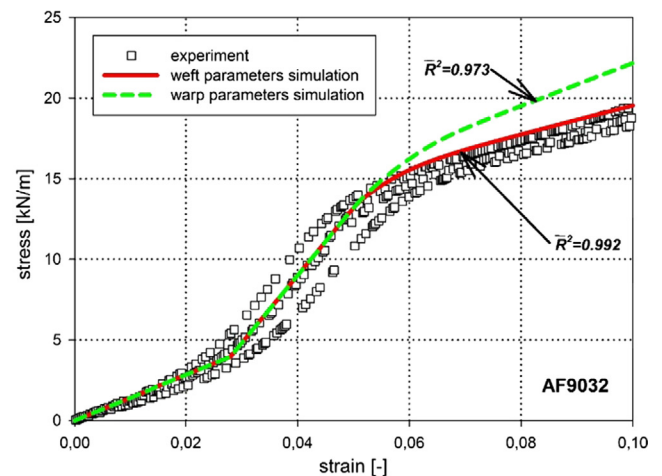
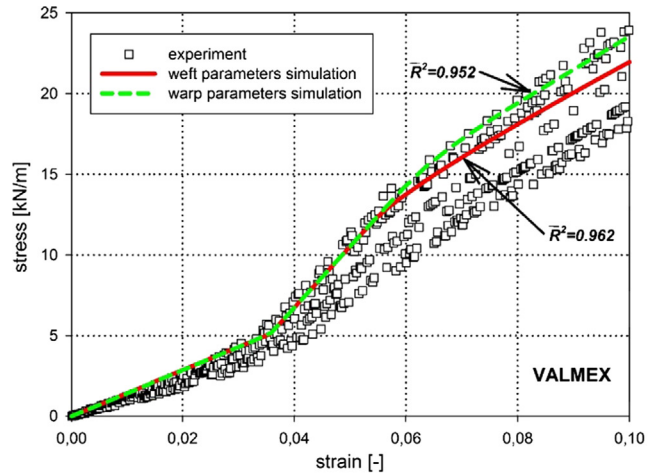
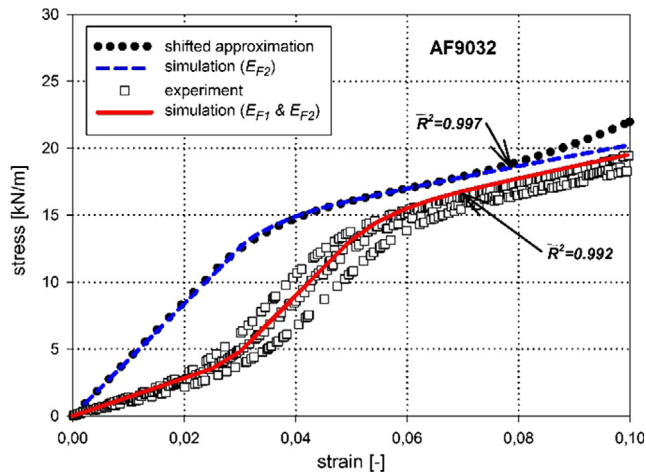
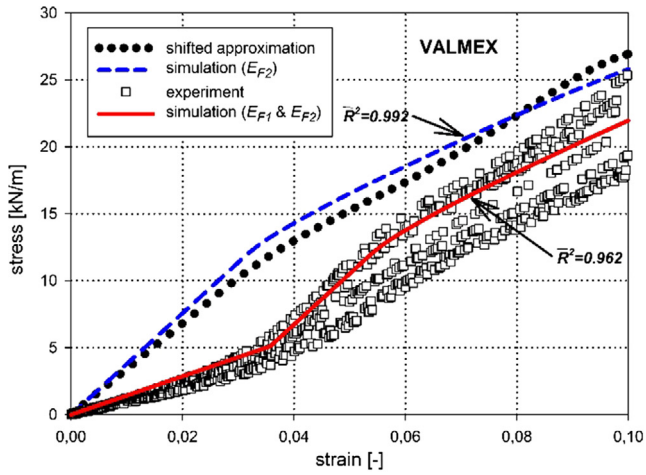


Fig. 9. Simulation results for the weft direction of the technical fabric VALMEX and AF9032 for strain rate of 0.0001 1/s.

Fig. 11. Comparison of the simulations using different parameters for the weft direction of the technical fabrics VALMEX and AF9032 for strain rate of 0.0001 1/s.

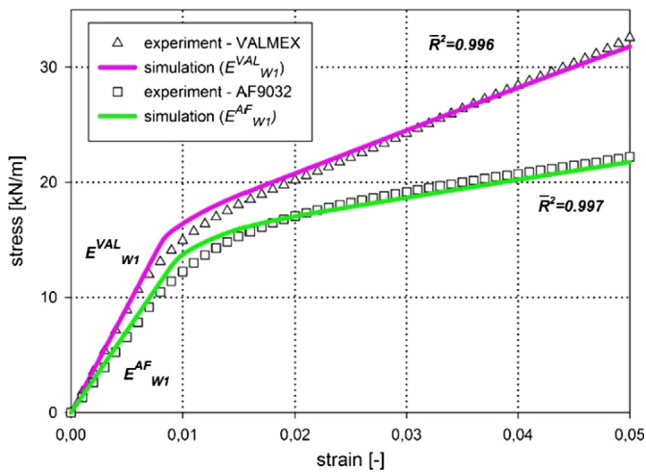


Fig. 10. Simulation results for the warp direction of the technical fabrics VALMEX and AF9032 for strain rate of 0.0001 1/s.

where pre-tensioning of the fabric is usually omitted and attention is focused on the durability parameters, e.g. ultimate tensile strength. In the second concept, both longitudinal stiffness coefficients are taken for the calculations. Therefore, the stress-strain graph is not shifted. This approach can also be presented in a simplified form with neglecting the first value of stiffness modulus and

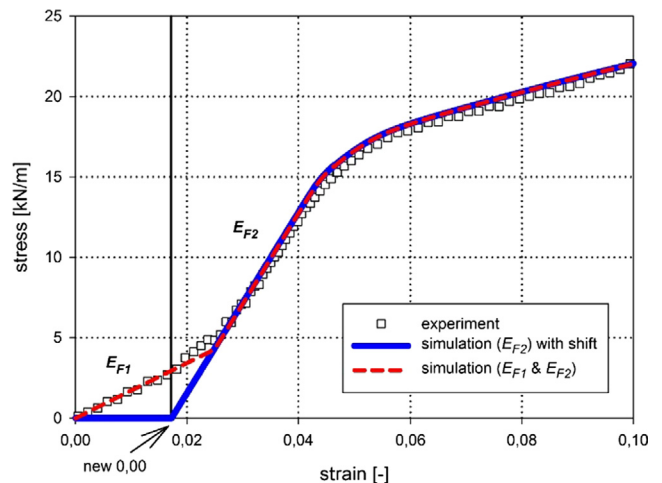


Fig. 12. Application comparison of the simulations for the weft direction of technical fabrics.

one, the stress-strain curve is shifted accordingly to the second stiffness modulus (true value of the longitudinal stiffness modulus). This approach seems to be mainly useful in the finite element calculations of structures strength, when stress limits are meaningful. Furthermore, the one-modulus concept would find wider application in the laboratory analysis of the textile materials,

taking the section initially used for shifting the experimental curves as the adopting phase, in which the weft threads undergo undulation (Fig. 12). After being fully stretched (at strain value of about 2%, with near zero stresses) the weft yarns start to carry subjected force. This approach presents the real behavior of the fabric under an initial stress state that is of the key importance during installation on a construction site and plays a great role in the final deflections of the geometry made of textiles.

6. Conclusions

In this work the technical fabrics mechanical properties described by the viscoplastic Bodner-Partom constitutive equations has been studied. The uniaxial tensile laboratory tests for the warp and weft direction has formed the basis for this analysis, as it has been proven before that for the PVC coated polyester fabrics (like AF9032 and VALMEX) direct results comparison of uniaxial and biaxial tensile tests is possible and their application gives similar effects in the FEM calculations of structures made of fabrics [24,3].

It has been confirmed that specific analysis is necessary to determine the parameters of constitutive equations for the warp and weft threads direction individually getting good convergences with the empirical data. The two approaches of the identification results for the weft direction have been proposed: the one-modulus and two moduli concept.

The authors managed to get the Bodner-Partom parameters not only for the warp, but also independently for the weft direction for both types of fabrics, as opposed to [16]. A new method of preliminary preparation of the laboratory tests has been presented. It has resulted in better correlation of the numerical and experimental functions for the weft direction of the fabric. It has been also confirmed that constitutive models developed for metals (like the Bodner-Partom model) can be successfully applied in the textile fabrics analysis.

Conflict of interest

There is no conflict of interest with any organization or person regarding the material discussed in the manuscript.

Acknowledgment

The author Krzysztof Żerdzicki would like to acknowledge Faculty of Civil and Environmental Engineering at Gdansk University of Technology, Poland (Grant GRAM for Krzysztof Żerdzicki) for the financial support of the research. The authors would like to thank the Polish Ministry of Science and Higher Education for sponsoring this research through the scholarship for young Polish researches and PhD students aimed to their scientific and developmental work in a year 2013/2014. Financial support from the French Government (Bourse du Gouvernement Français) is also greatly acknowledged.

References

- [1] Ambroziak A, Kłosowski P. Mechanical properties of polyvinyl chloride-coated fabric under cyclic tests. *J Reinf Plast Compos*. <http://dx.doi.org/10.1177/0731684413502858>.
- [2] Ambroziak A, Kłosowski P. Review of constitutive models for technical woven fabrics in finite element analysis. *AATCC Rev* 2011;11(3):58–67.
- [3] Ambroziak A, Kłosowski P. Mechanical properties for preliminary design of structures made from PVC coated fabric. *Constr Build Mater* 2014;50:74–81.
- [4] Andersson H. An implicit formulation of the Bodner-Partom constitutive equations. *Comput Struct* 2003;81:1405–14.
- [5] Bles G, Nowacki WK, Tourabi A. Experimental study of the cyclic visco-elasto-plastic behaviour of a polyamide fibre strap. *Int J Solids Struct* 2009;46:2693–705.
- [6] Bodner SR, Partom Y. Constitutive equations for elastic-viscoplastic strain-hardening materials. *J Appl Mech* 1985;42:385–9.
- [7] Bodner SR. Evolution equations for anisotropic hardening and damage of elastic-viscoplastic materials. In: Sączak A, Biandisi G, editors. *Plastic today*. Barking: Elsevier; 1985. p. 471–82.
- [8] Bodner SR. Unified plasticity – an engineering approach. Final report. Faculty of Mechanical Engineering, Technion – Israel Institute of Technology Haifa; 2000.
- [9] Boisse P, Buet K, Gasser A, Launay J. Meso/macro-mechanical behavior of textile reinforcements for thin composites. *Compos Sci Technol* 2001;61(3):395–401.
- [10] Branicki CZ, Kłosowski P. Static analysis of hanging textile membranes in nonlinear approach. *Arch Civil Eng* 1983;XXIX/3:189–220 [in Polish].
- [11] Chan KS, Bodner SR, Lindholm US. Phenomenological modeling of hardening and thermal recovery in metals. *J Eng Mater Technol* 1988;110:1–8.
- [12] Huang S, Khan AS. Modeling the mechanical behavior of 1100–0 aluminum at different strain rates by the Bodner-Partom model. *Int J Plast* 1992;8:501–12.
- [13] ISO 1421:2001. Fabrics coated with rubber or plastics – determination of breaking strength and elongation at break.
- [14] Kim JK, Yu WR, Kim SM. Anisotropic creep modeling of coated textile membrane using finite element analysis. *Compos Sci Technol* 2008;68:1688–96.
- [15] King MJ, Jearanaisilawong P, Socrate S. A continuum constitutive model for the mechanical behavior of woven fabrics. *Int J Solids Struct* 2005;42:3867–96.
- [16] Kłosowski P, Zagubień A, Woźnica K. Investigation on rheological properties of technical fabric “Panama”. *Arch Appl Mech* 2004;73:661–81.
- [17] Kłosowski P, Mleczek A. Identification of Bodner-Partom viscoplastic model parameters for some aluminium alloys at elevated temperature. [http://dx.doi.org/10.1061/\(ASCE\)MT.1943-5533.0001875](http://dx.doi.org/10.1061/(ASCE)MT.1943-5533.0001875).
- [18] Komeili M, Milani AS. The effect of meso-level uncertainties on the mechanical response of woven fabric composites under axial loading. *Comput Struct* 2012;90–91:163–71.
- [19] Kumazawa H, Susuki I, Morita T, Kuwabara T. Mechanical properties of coated plain weave fabrics under biaxial loads. *Trans Jpn Soc Aero Space Sci* 2005;48(160):117–23.
- [20] Mazza E, Papes O, Rubin MR, Bodner SR, Binur NS. *Biomech Modell Mechanobiol* 2005;4(2–3):178–89.
- [21] Moreno V, Jordan EH. Prediction of material thermomechanical response with a unified viscoplastic constitutive model. *Int J Plast* 1986;2:223–45.
- [22] Potluri P, Thammandra VS. Influence of uniaxial and biaxial tension on meso-scale geometry and strain fields in a woven composite. *Compos Struct* 2007;77:405–18.
- [23] Realf ML, Boyce MC, Backer S. A micromechanical model of the tensile behavior of woven fabric. *Text Res J* 1997;67(6):445–59.
- [24] Reinhardt HW. On the biaxial testing and strength of coated fabrics. *Exp Mech* 1976;16(2):71–4.
- [25] Rubin MB, Bodner SR. A three-dimensional nonlinear model for dissipative response of soft tissue. *Int J Solids Struct* 2002;39(19):5081–99.
- [26] Sands CM. Rapid implementation of material models within finite element analysis. *Comput Mater Sci* 2009;47:286–96.
- [27] Seaman RN, Bradenburg F. Utilization of vinyl-coated polyester fabrics for architectural applications. - Part 1. Fabric architecture; 2000.
- [28] Woźnica K, Kłosowski P. Evaluation of viscoplastic parameters and its application for dynamic behaviour of plates. *Arch Appl Mech* 2000;70:561–70.
- [29] Xue P, Peng X, Cao J. A non-orthogonal constitutive model for characterizing woven composites. *Composites: Part A* 2003;34:183–93.
- [30] Zaïri F, Nait-Abdelaziz M, Woźnica K, Gloaguen JM. Constitutive equations for the viscoplastic-damage behaviour of a rubber-modified polymer. *Eur J Mech A/Solids* 2005;24:169–82.

